Nonconfocal Multimode Resonators for Masers*

R. F. SOOHOO†, SENIOR MEMBER, IRE

Summary—**The case of a resonator composed of two concave spherical reflectors separated by an arbitrary distance is examined. The general problem of the electromagnetic field distribution over the nonconfocal aperture is first formulated by means of the Huygens principle. The solution of the resulting integral equation is obtained analytically in the highly nonconfocal limit. It was found that when the reflector spacing d is much larger than the radius of curvature b of the reflectors, the aperture field distribution is in the form of traveling waves.**

For arbitrary d/b, the eigenvalues and eigenfunctions of the lowest order mode is obtained by numerical solution using the IBM 7090 computer. The diffraction loss was found to increase rapidly when $d \rightarrow 2b$ and a geometrical interpretation of this behavior is given. Furthermore, it was found that as the spacing departs from the confocal value, the apertures are no longer surfaces of constant phase. The optimum spacing for maximum Q of the resonator is also obtained.

I. Introduction

AT ULTRAMICROWAVE through optical frequencies, the wavelengths are of the order of 10^{-1} to 10^{-4} cm. Thus, in order to achieve reasonable physical dimensions and high Q, resonators for masers operating at these frequencies must, of necessity, be of the multimode type. This is in contrast to the situation at microwave frequencies ($\lambda \sim 1$ cm) where cavities may be of such convenient physical dimensions as to substain only the dominant mode.

Schawlow and Townes,[1] Prokhorov,[2] and Dicke[3] have suggested the use of the Fabry-Perot interferometer,[4] composed of two reflecting plates separated by an arbitrary distance, as resonator for infrared and optical masers. Such open structures have two sources of loss: diffraction loss due to the escaping of energy out of the region between the two plates, and the losses due to absorption in and transmission through the reflectors. Although the losses of a parallel plate resonator are reasonably small, its configuration is, however, not one that yields the highest possible Q. A resonator formed by two identical spherical reflectors separated by their radius of curvature has been shown to give diffraction losses that are orders of magnitude lower than that of the parallel plane resonator.[5,6] Since the focal length of a spherical reflector is one half its radius of curvature, the focal points of the reflectors are coincident and the resonators are therefore termed confocal. Intuitively, we might think of the shape of the spherical surfaces as being more effective in confining the energy between them than are two parallel plates, thus giving rise to lower diffraction losses. The use of confocal spherical reflectors as an interferometer has been described by Connes.[7] In contrast with the case of the Fabry-Perot interferometer, it has been found that parallelism between the spherical reflectors is not a strict requirement; the only fine adjustment required being the spacing between the reflectors.

In this paper, we shall study mathematically and physically the behavior of the resonator when its spherical reflectors are separated by an arbitrary distance. Such analysis of the nonconfocal resonator would yield the eigenvalues and eigenfunctions of the resonator from which the diffraction losses may be computed as a function of the arbitrary reflector separation d. The results of this analysis would enable us to examine, among other things, the effect upon the behavior of a maser employing spherical reflectors due to longitudinal misalignment between the reflectors (*i.e.*, due to slight departure from confocal spacing). Furthermore, since the diffraction losses should increase with increasing reflector separation above the confocal value while the Q due to reflections may be expected to increase with increasing d for small diffraction loss, it should be possible to determine the optimum value of d for maximum Q from our analysis.

II. Formulation of Problem

Consider the resonator configuration as shown in Fig. 1. Assuming that the square aperture dimension $2a$ and reflector separation d are all small compared with the wavelength λ, we may use the Huygens-Fresnel principle in the zero wavelength limit. The analysis using this principle yields an expression for E_y by summing contributions from all the differential Huygens sources dis-

* Received August 13, 1962.

† Department of Electrical Engineering, California Institute of Technology, Pasadena, Calif.

[1] A. L. Schawlow and C. H. Townes, "Infrared and optical masers," *Phys. Rev.*, vol. 112, pp. 1940–1949; December, 1958.

[2] A. M. Prokhorov, "Molecular amplifier and generator for submillimeter waves," *Soviet Physics JETP* (Translation), vol. 7, pp. 1140–1141; December, 1958.

[3] R. H. Dicke, U. S. Patent No. 2,851,652; Sept. 9, 1958.

[4] K. W. Meissner, "Interference spectroscopy," *J. Opt. Soc. Am.*, pt. I, vol. 31, pp. 405–427; June, 1941; pt. II, vol. 32, pp. 185–211; April, 1942.

[5] G. D. Boyd and J. P. Gordon, "Confocal multimode resonators for millimeter through optical wavelength masers," *Bell Sys. Tech. J.*, vol. 40, pp. 489–508; March, 1961.

[6] A. G. Fox and T. Li, "Resonant modes in a maser interferometer," *Bell Sys. Tech. J.*, vol. 40, pp. 469–473; March, 1961.

[7] P. Connes, "Increase of the product of luminosity × resolution with interferometers by employing path differences independent of incidence," *Revue d'Optique*, vol. 35, pp. 37–42; January, 1956; "L'etalon, de Fabry-Perot spherique," *J. Phys. Radium*, vol. 19, pp. 262–269; March, 1958.

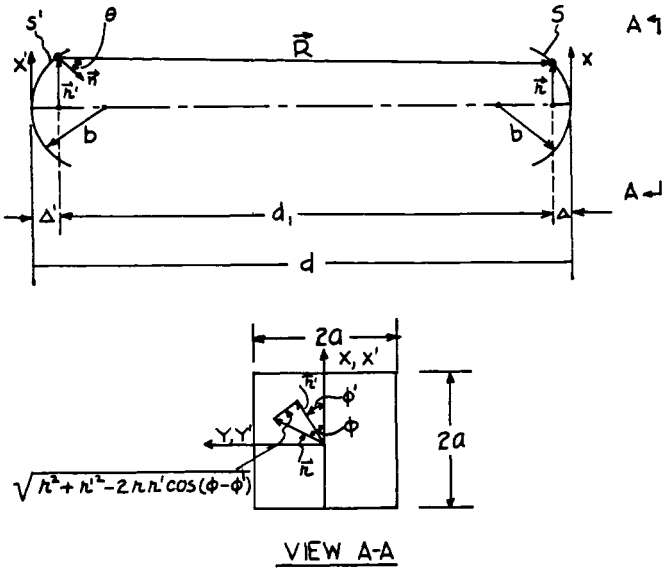

Fig. 1—Nonconfocal resonator with spherical reflectors.

tributed over the left reflector surface S':[8]

$$E_y = \int_{S'} \frac{ik(1+\cos\theta)}{4\pi R} e^{-ikR} E_0 f_m(x') g_n(y') ds' \qquad (1)$$

where $k = 2\pi/\lambda$ is the wave number and θ is the angle between the surface normal $\boldsymbol{n}$ and $\boldsymbol{R}$. Since $a/d \ll 1$, $\theta \to 0$ and $\cos\theta$ approaches unity. $E_0 f_m(x') g_n(y')$ represents the electric field at r' on the left reflector surface S' and is assumed to be linearly polarized in the y-direction. It may be noted that $e^{i(\omega t - kR)}/4\pi R$ represents the familiar amplitude and phase dependence on t and R of a radiation field emanating from a dipole.

The eigenfunctions of the nonconfocal resonator can be obtained by solving (1) with $E_y = E_1 f_m(x) g_n(y)$ thus requiring that the field distribution over $x'y'$ reproduce itself over the xy aperture within a constant. It follows from (1) that

$$\sigma_m \sigma_n f_m(x) g_n(y) = \int_{-a}^{+a} \int_{-a}^{+a} \frac{ik}{2\pi R} e^{-ikR} f_m(x') g_n(y') dx' dy' \qquad (2)$$

where $\sigma_m \sigma_n = E_1/E_0$ is the eigenvalue belonging to the eigenfunction $f_m(x) g_n(y)$ and is in general complex. Thus $f_m(x) g_n(y)$ represents the electromagnetic field distribution over the xy aperture while $\sigma_m \sigma_n$ is related to the phase shift and diffraction loss of the normal mode mn. Note that if it were not for diffraction losses, the amplitude of the reflected wave from the right surface $S(E_1)$ would be exactly equal to $+E_0$ or $-E_0$ making $\sigma_m \sigma_n = \pm 1$.

Now, let ϕ' and ϕ be the angle between x' and r' and between x and r, respectively. Then, it follows from the geometrical configuration of Fig. 1 that

$$R = \sqrt{d_1^2 + r^2 + r'^2 - 2rr'\cos(\phi - \phi')} \qquad (3)$$

and

$$\Delta = b - \sqrt{b^2 - r^2} \simeq \frac{r^2}{2b} \qquad (4)$$

$$\Delta' = b - \sqrt{b^2 - r'^2} \simeq \frac{r'^2}{2b} \qquad (5)$$

$$d_1 = d - \Delta - \Delta' \qquad (6)$$

where b is the radius of curvature of the reflectors. Combining (4)–(6), we have an expression for d_1 in terms of d, b, r, and r'. Substituting this expression for d_1 into (3) and keeping in mind that $a/d \ll 1$, we find by the binomial expansion the approximate expression for R as

$$R \simeq d - \frac{xx' + yy'}{d^2} - \frac{d-b}{2bd}(x^2 + x'^2 + y^2 + y'^2). \qquad (7)$$

Since $a/d \ll 1$, we may replace R by d in (1) except in the exponential phase term e^{-ikR} where we would use expression (7) for R. Thus, (1) becomes

$$\begin{aligned}\sigma_m \sigma_n F_n(X) G_n(Y) &= \frac{ie^{-ikd}}{2\pi} \int_{-\sqrt{c}}^{+\sqrt{c}} F_m(X') \cdot \exp[iXX'] \exp\left[i\frac{d-b}{2b}(X^2 + X'^2)\right] dX' \\ &\times \int_{-\sqrt{c}}^{+\sqrt{c}} G_n(Y') \cdot \exp[iYY'] \exp\left[i\frac{d-b}{2b}(Y^2 + Y'^2)\right] dY' \end{aligned} \qquad (8)$$

where we have introduced the dimensionless variables similar to those used by Boyd and Gordon[5] in their analysis of the confocal resonator

$$c = \frac{a^2 k}{d} = 2\pi \frac{a^2}{d\lambda}$$
$$X = \frac{x\sqrt{c}}{a} \qquad Y = \frac{y\sqrt{c}}{a}. \qquad (9)$$

When $d = b$, Boyd and Gordon point out that (8) is a homogeneous Fredholm equation of the second kind with $e^{iXX'}$ as the kernel and its solution has been considered by Flammer,[9] Slepian and Pollak.[10] In the general nonconfocal case considered here, the kernel

$$\exp[iXX'] \exp\left[i\frac{d-b}{2b}(X^2 + X'^2)\right]$$

[8] S. Silver, "Microwave Antenna Theory and Design," M.I.T. Rad. Lab. Ser., McGraw-Hill Book Company, Inc., New York, N. Y., vol. 12, p. 118; 1949.

[9] C. Flammer, "Spherical Wave Functions," Stanford University Press, Stanford, Calif.; 1957.

[10] D. Slepian and H. O. Pollak, "Prolate spheroidal wave functions, Fourier analysis and uncertainty—I," *Bell. Sys. Tech. J.*, vol. 40, pp. 43–64; January, 1961.

is more complicated and we shall resort to both analytical and numerical solution as discussed in the following sections.

III. Analytical Solution

Eq. (8) may be written as a pair of equations

$$\chi_m F_m(X) = \frac{1}{\sqrt{2\pi}} \int_{-\sqrt{c}}^{+\sqrt{c}} F_m(X') \cdot \exp[iXX'] \exp\left[i \frac{d-b}{2b}(X^2 + X'^2)\right] dX' \quad (10)$$

and

$$\chi_n G_n(Y) = \frac{1}{\sqrt{2\pi}} \int_{-\sqrt{c}}^{+\sqrt{c}} G_n(Y') \cdot \exp[iYY'] \exp\left[i \frac{d-b}{2b}(Y^2 + Y'^2)\right] dY' \quad (11)$$

where $\chi_m \chi_n = \sigma_m \sigma_n / ie^{-ikd}$. Since (10) and (11) are identical in form, we need henceforth consider one of them, say (10), only.

The exact solution of (10) is rather complicated. Therefore, before we discuss its general solution using numerical methods in Section IV, it would be instructive to consider its solution in some limiting cases. The two limiting cases of obvious interest are: 1) the exactly confocal case ($d=b$) and 2) the highly nonconfocal case ($d \gg b$).

First, let us consider the confocal case. In this limit, (10) becomes

$$\chi_m F_m(X) = \frac{1}{\sqrt{2\pi}} \int_{-\sqrt{c}}^{+\sqrt{c}} F_m(X') e^{iXX'} dX'. \quad (12)$$

The eigenfunctions and eigenvalues of (12) have been shown to be,[10,5]

$$F_m(c, \eta) \alpha S_{0m}(c, \eta) \quad (13)$$

$$\chi_m = \sqrt{\frac{2c}{\pi}}\, i^m R_{0m}^{(1)}(c, 1) \qquad m = 0, 1, 2, \quad (14)$$

where $S_{0m}(c, \eta)$ and $R_{0m}^{(1)}(c, 1)$ are, respectively, the angular and radial wave functions in prolate spheroidal coordinates as defined by Flammer,[9] and where $\eta = X/\sqrt{c} = x/a$. For a given value of c, the eigenfunction $F_m(c, \eta)$ may be plotted as a function of η and the eigenvalue of F_m may likewise be evaluated. In Fig. 2, $F_0(c, \eta)$, the electric field distribution of the lowest order mode, has been plotted as a function of η for $c=5$. It is seen that the field decays in amplitude as we move away from the center of the aperture. Since the eigenfunctions $F_m(c, \eta)$ are real, the aperture represents a surface of constant phase [see Fig. 3]. As c increases, $F_0(c, \eta)$ decays even more rapidly with increasing η.[5]

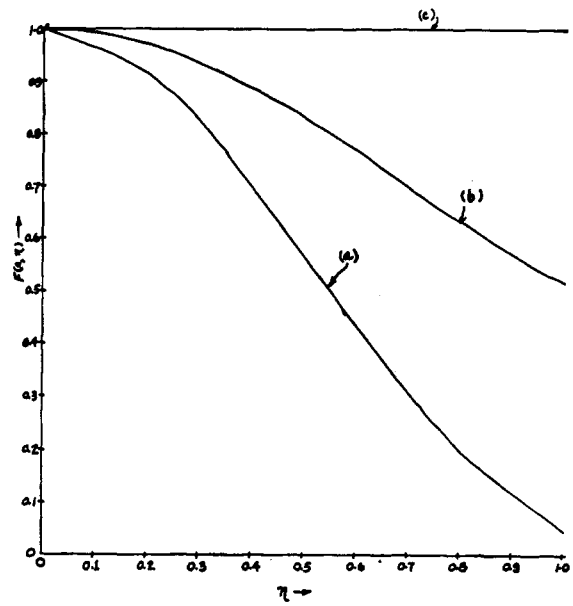

Fig. 2—Relative electric field amplitude vs normalized spacing from center of aperture for (a) $d/b=1$, (b) $d/b=2$, and (c) $d/b \gg 1$.

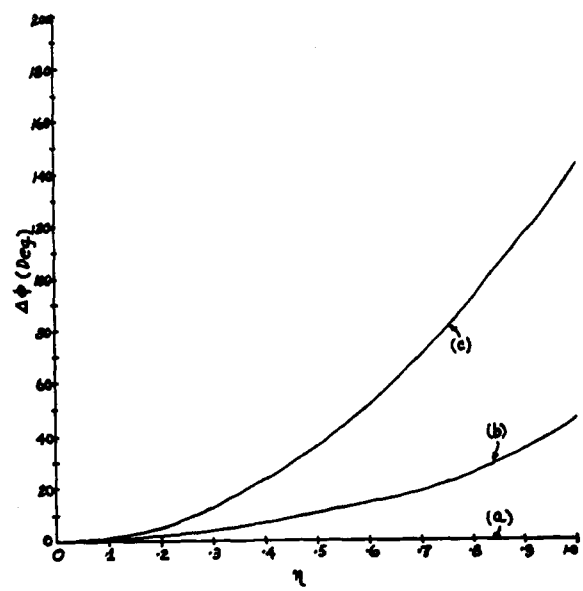

Fig. 3—Relative phase of the electric field vs normalized spacing from center of aperture for (a) $d/b=1$, (b) $d/b=2$, and (c) $d/b \gg 1$.

Next, let us consider the highly nonconfocal case where the ratio d/b is sufficiently large so that

$$\frac{d-b}{2b}(X^2 + X'^2) \gg XX' \quad (15)$$

and $e^{iXX'}$ is close to unity for all possible values of X'. Then, (10) becomes

$$\chi_m F_m(X) \simeq \frac{1}{\sqrt{2\pi}} \int_{-\sqrt{c}}^{+\sqrt{c}} F_m(X') e^{i(d/2b)(X^2+X'^2)} dX' = \frac{1}{\sqrt{2\pi}} e^{i(d/2b)X^2} \int_{-\sqrt{c}}^{+\sqrt{c}} F_m(X') e^{i(d/2b)X'^2} dX'. \quad (16)$$

Since the integrand in the last expression of (16) is independent of X as $F_m(X')$ is independent of X, the integral must integrate to some constant independent of X which could only influence the eigenvalue χ_m but not $F_m(X)$. By examining the factor $e^{i(d/2b)X^2}$ in (16), we conclude that

$$F_m(X) \simeq e^{i(d/2b)X^2} \tag{17}$$

when d is sufficiently large. The form (17) implies an inward traveling wave at the aperture and is plotted in Figs. 2 and 3 as a function of η.

Putting expression (17) into (16), we easily evaluate the definite integral as $c\to\infty$ or $\lambda\to 0$ giving the eigenvalue χ_m as

$$\chi_m = \frac{(1+i)}{2\sqrt{\frac{d}{b}}}. \tag{18}$$

It follows that the diffraction loss α_D is

$$\alpha_D = 1 - |\sigma_m\sigma_n|^2 = 1 - |\chi_m\chi_n ie^{-ikd}|^2$$
$$= 1 - |\chi_m\chi_n|^2 \tag{19}$$

or equal to $1-(b/2d)^2$. Actually, (16) could be evaluated when d is large for any value of c by the method of stationary phase (see Appendix) giving the same result for χ_m as (18).

It is instructive to reconsider the limit (15). We find by simple algebraic manipulation that

$$d \gg b + \frac{2b}{\frac{X}{X'} + \frac{X'}{X}}. \tag{20}$$

Since the minimum value of $X/X'+X'/X$ occurs when $X=\pm X'$, we find (20) implies that the point

$$d = 2b$$

is a transition point of interest. This situation may be subjected to a geometrical interpretation as depicted in Fig. 4.

Consider Fig. 4(a) where we have depicted the path of the light rays for the highly nonconfocal resonator. Light rays a' and a'' parallel to the resonator axis incident upon the left reflector will be reflected and converge on the focal point of the left reflector. Of course, due to diffraction, the light beam will actually spread somewhat as it is reflected from the left reflector and travels toward the right. It is seen from Fig. 4 that energy reflected from the surface S' will be captured by the right side reflector while energy reflected from the surface outside S' will not be intercepted by it. From energy balance considerations, we easily see that:

$$\alpha_D = \frac{\text{Energy Loss}}{\text{Total Energy}} = 1 - \frac{\text{Energy Confined}}{\text{Total Energy}}. \tag{21}$$

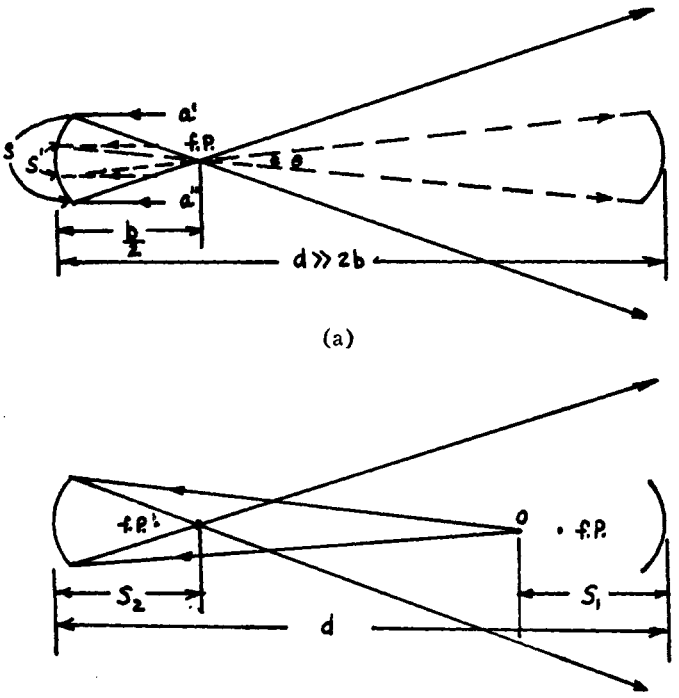

Fig. 4—Geometrical interpretation of diffraction loss for (a) $d/b\gg 1$ (highly nonconfocal) and (b) $d\backsim b$.

For $d\gg 2b$, we have from Fig. 4(a):

$$\alpha_D = 1 - \frac{S'}{S} = 1 - \frac{\left(\frac{b}{2}\theta\right)^2}{(2a)^2}. \tag{22}$$

But, $\theta\cong 2a/d$ when $d\gg b$. Thus Eq. (22) becomes

$$\alpha_D = 1 - \left(\frac{b}{2d}\right)^2 \tag{23}$$

which is identical to (19) obtained by a more sophisticated mathematical procedure.

When d is not much larger than b, we cannot consider the light source as located at infinity producing rays a' and a'' parallel to the axis. We then have the situation in Fig. 4(b) where light rays a' and a'' originate from some point 0 on the axis. We can similarly show that $\alpha_D = 1-(S_2/d-S_2)^2$. Noting that $S_1=S_2$ for symmetrical case and $1/f=2/b=1/S_1+1/S_2$ where f is the focal length, we find that α_D is zero up to $d=2b$ where it begins to increase abruptly. Thus, this idealized geometrical analysis indicates that $d=2b$ is a transition point of interest consistent with the limit (20) previously found.

Numerical Solution

The equation

$$F_m(X) = \frac{1}{\chi_m\sqrt{2\pi}}\int_{-\sqrt{c}}^{+\sqrt{c}} F_m(X')e^{iXX'}e^{i(d-b)/2b(X^2+X'^2)}dX' \tag{24}$$

is a homogeneous Fredholm equation of the second kind with the kernel

$$K(X, X') = e^{iXX'}e^{i(d-b)/2b(X^2+X'^2)}.$$

Letting $F_{mi}=F_m(X_i)$ and $K_{ij}=K(X_i, X_j')$, (24) can be approximated by

$$F_{mi} = \frac{h}{\chi_m\sqrt{2\pi}} \sum_{j=0}^{n} (A_jK_{ij}F_{mj}) \tag{25}$$

where we have divided the interval $-\sqrt{c}\leq X\leq+\sqrt{c}$ into n equal parts by the points

$$X_i = -\sqrt{c} + jh \qquad j = 0, 1, 2 \cdots n. \tag{26}$$

The weights A_j will depend on the particular quadrature formula used. For the most widely used Simpson's rule

$$A_j = \frac{1}{3}, \frac{4}{3}, \frac{2}{3}, \frac{4}{3}, \frac{2}{3}, \cdots \frac{4}{3}, \frac{1}{3},$$

letting $H_{ij}=hA_jK_{ij}$, (25) represent a set of linear equations

$$F_{mi} = \frac{1}{\chi_m\sqrt{2\pi}} \sum_{j=0}^{n} (H_{ij}F_{mj}) \tag{27}$$

where (27) is a finite difference approximation to the integral operation of (24).

If we consider the numbers F_{mi} as components of the vector $\boldsymbol{F}_{mi}$, the set of equations (24) can be written concisely in the form

$$\sqrt{2\pi}\,\chi_m\boldsymbol{F}_m = H\boldsymbol{F}_n \tag{28}$$

where $H=|H_{ij}|$ is a matrix with components i, j. Eq. (28) is thus, just the familiar eigenvalue equation. Numerical methods may be used to solve (28) for the eigenfunction F_m and the eigenvalue χ_m by iteration.[11] This has been done by the IBM 7090 computer and the results are presented in the next section.

IV. Numerical Results

As enumerated in Section III, the fractional energy loss per reflection due to diffraction effects is given by

$$\alpha_D = 1 - |\sigma_m\sigma_n|^2 = 1 - |\chi_m\chi_n|^2 \tag{29}$$

with $\sigma_m\sigma_n=\chi_m\chi_n ie^{-ikd}$. The values of α_D obtained by the numerical solution of (28) is plotted as a function of d/b for the lowest-order mode ($m=n=0$) with $c=5/(d/b)$. It is seen that the diffraction loss remains quite low until $d\rightarrow 2b$ where it begins to increase rather rapidly toward the final value of unity as $d/b\rightarrow\infty$. This behavior is consistent with the results of the section on analytical solution. Thus, as d departs from the confocal value and increases without limit, we find from Figs. 2 and 3 that the normal modes of the resonator change from a standing-wave distribution across the reflector aperture with most of the energy confined between them in the manner of a closed resonator to an inward traveling wave at the aperture. This traveling wave carries most of the energy away from the resonator giving rise to high diffraction loss as evidenced by Fig. 4(a). Since the eigenfunction in the limiting case of $d/b\rightarrow\infty$ is given by $e^{i(d/2b)(X^2+Y^2)}$ according to (17), contours of constant phase are circles centered about the axis of the aperture.

The phase shift between two confocal reflectors equals the phase angle of $\sigma_m\sigma_n$ as the reflectors are then surfaces of constant phase since the eigenfunctions are real. Under this condition, the round trip phase shift of the electromagnetic field must be equal to an integer q times 2π for resonance to occur. Thus, the normal modes of the resonator are composed of a triply infinite set each designated by the integer numbers m, n, q. As the separation between the reflectors d departs from the confocal value b, however, the eigenfunctions become complex and the apertures are no longer surfaces of constant phase. This is illustrated in Figs. 2 and 3 where we have plotted the amplitude and phase of $F_m(X)$ as a function of η for $d/b=2$ for comparison with those of the confocal and highly nonconfocal cases.

V. Discussion

It has been shown that as the separation between reflectors d departs from the confocal value b, there will be a finite phase shift across the aperture. This in turn implies that the resonances for different normal modes of the resonator are no longer infinitely sharp even for perfectly conducting reflectors assumed in this paper. However, as illustrated in Fig. 5 the phase shift across the aperture is small until $d\rightarrow 2b$. Thus, so long as d is sufficiently less than $2b$, the line broadening due to the phase shift across the aperture should not severely influence the behavior of a maser using this type of resonator.

Since the diffraction loss is seen to be extremely low at confocal spacing (about 2×10^{-3} from Fig. 6), it may be possible to increase the Q of the resonator by increasing the separation d beyond the confocal value as the Q due to reflector losses should increase with increasing d for small diffraction loss. The maximum Q should occur for the value of d giving approximately equal reflection and diffraction losses. Thus, for the case in point, *i.e.*, $c=5/(d/b)$, the optimum d/b for maximum Q should be about 1.5 according to Fig. 6 for a reflection loss of 1 per cent. Indeed, we would expect the optimum value of d/b be between 1 and 2 for any reasonable value of c.

Neither the diffraction loss nor the phase shift across the aperture changes rapidly about the position $d/b=1$ according to Figs. 4 and 6. Thus, slight longitudinal misalignment of the reflectors should not have a critical effect upon maser operation.

[11] J. N. Franklin, "Computation of Eigenvalues by the Method of Iteration," Calif. Inst. Tech., Pasadena, Calif., Computing Center Tech. Rept. No. 111; Oct., 1957.

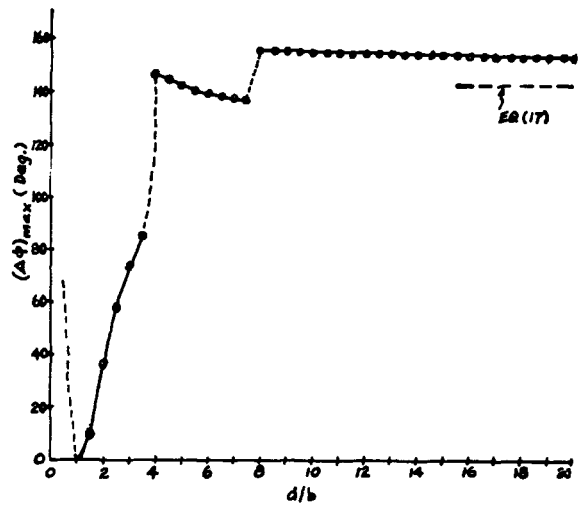

Fig. 5—Maximum phase shift across reflector aperture vs d/b.

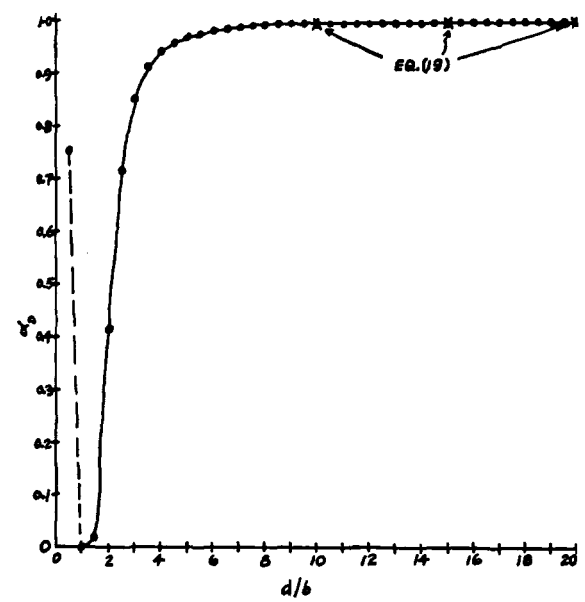

Fig. 6—Diffraction loss of nonconfocal resonator vs d/b.

Appendix

With $F_m(X') = e^{i(d/2b)X'^2}$, Eq. (16) becomes:

$$\chi_m F_m(X) = \frac{e^{i(d/2b)X^2}}{\sqrt{2\pi}} \int_{-\sqrt{c}}^{+\sqrt{c}} e^{i(d/b)X'^2} dX'. \tag{30}$$

In the limit where $c \to \infty$, the integral may be easily evaluated as indicated in the text. However, if c is finite as is always the case, the integral could still be evaluated to an accuracy of the order of (b/d) by the method of stationary phase.[12] The method is based upon recognizing the fact that in a wave problem of this kind, the contributions from parts of the range of integration near a point of stationary phase will be nearly in phase and add up, whereas those from other parts will interfere. Let $\psi(X') = X'^2 = \theta$, then (30) becomes

$$\chi_m F_m(X) = \frac{e^{i(d/2b)X^2}}{\sqrt{2\pi}} \int_{X'=-\sqrt{c}}^{X'=+\sqrt{c}} \frac{1}{\psi'(X')} e^{i(d/b)\theta} d\theta. \tag{31}$$

According to (31), the saddle point of $\psi(X')$, namely, the point about which we have the most contribution to the integral is

$$\psi'(X') = 2X' = 0. \tag{32}$$

Consider now the integral from $(0-\delta)$ to $(0+\delta)$, letting

$$\psi(X') - \psi(0) = u^2 \simeq \tfrac{1}{2}\psi''(0)(X' - 0)^2. \tag{33}$$

We have

$$I_\delta = \frac{e^{i(d/2b)X^2}}{\sqrt{2\pi}} \int_{X'=-\delta}^{X'=+\delta} \frac{1}{\psi'(X')} 2ue^{i(d/b)[\psi(0)+u^2]} du. \tag{34}$$

Let $A_0 = [2u/\psi'(X')]_{X'=0}$, then

$$I_\delta = \frac{e^{i(d/2b)X^2}}{\sqrt{2\pi}} \int_{X'=-\delta}^{X'=+\delta} \left\{ A_0 e^{i(d/b)[\psi(0)+u^2]} + \left[\frac{2u}{\psi'(X')} - A_0\right] e^{i(d/b)[\psi(0)+u^2]} \right\} du. \tag{35}$$

It can be shown that the magnitude of the second part of the integral is of the order b/d.[12] Thus,

$$I_\delta = \frac{e^{i(d/2b)X^2}}{\sqrt{2\pi}} \int_{X'=-\delta}^{X'=+\delta} e^{i(d/b)u^2} du + 0\left(\frac{b}{d}\right) \tag{36}$$

where we have evaluated A_0. The integral is a Frensnel integral of complex argument and is equal to

$$e^{i(\pi/4)} \sqrt{\frac{\pi b}{d}} + 0\left(\frac{b}{d}\right).$$

Combining (30) and (36), we easily find the eigenvalue χ_m as

$$\chi_m \simeq \frac{(1+i)}{2\sqrt{\frac{d}{b}}} \tag{37}$$

which is identical with that given by (18) in the text, obtained in the limit where $c \to \infty$.

Acknowledgment

The author wishes to thank Dr. N. George for illuminating discussions and Drs. N. Franklin and K. Hebert for aid in numerical computation.

[12] H. Jeffreys and B. S. Jeffreys, "Methods of Mathematical Physics," Cambridge University Press, Cambridge, England, 2nd ed., pp. 505–406; 1950.